Ab initio molecular dynamics description of proton transfer at water-tricalcium silicate interface

J. Claverie, Fabrice Bernard, J.M.M. Cordeiro, Siham Kamali-Bernard

ab initio molecular dynamics description of proton transfer at water-tricalcium silicate interface

Jérôme Claverie[a,b], Fabrice Bernard[a], João Manuel Marques Cordeiro[b], Siham Kamali-Bernard[a]

[a] *Laboratory of Civil Engineering and Mechanical Engineering (LGCGM), INSA Rennes, Rennes, France*
[b] *Department of Physics and Chemistry, School of Natural Sciences and Engineering, São Paulo State University (UNESP), 15385-000 Ilha Solteira, São Paulo, Brazil*

Abstract

For the first time, an *ab initio* molecular dynamics simulation was performed to describe the C_3S/water interface. The simulation shows that oxides with favorable environment are protonated at first, creating very stable hydroxide groups. Proton transfers occur between water and silicates, and between water and hydroxides formed upon water dissociation on the surface. The typical lifetime of these events is on the same timescale than interconversion between Eigen and Zundel ions in bulk water. At the very early stage of the hydration encompassed by our simulation, silanol groups are very unstable and molecular adsorption of water is slightly more stable than dissociative adsorption.

Keywords: Tricalcium silicate. Hydration. *ab initio* Molecular Dynamics. Proton transfer. Interface.

1. Introduction

Although the use of low clinker ratio cements is increasing, the development of new clinker types remains a reliable strategy to reduce greenhouse gas emissions and improve the properties of cement for concrete structures applications. In a context of durable design, considerable efforts are being made for a better understanding of original Portland cement (OPC) hydration. However, considering the hydration of all clinker phases together would turn the study highly complex. Most of the time, the tricalcium silicate (C_3S) received a particular attention, due to its predominance in OPC clinker (about 50 % to 70 % by mass). C_3S is the main phase responsible for OPC setting and strength development. The reactivity and early hydration of tricalcium silicate (C_3S) is a very relevant topic towards a more sustainable design of OPC. The hydration itself encompasses several processes such as dissolution, phase growth, diffusion and complexation [1]. Atomistic simulation methods have shown good capabilities in predicting the reactivity of mineral surfaces and the behavior of solid/liquid interfaces. Towards a better understanding of the phases and processes occurring in cementitious systems, many atomistic force fields have been optimized [2]. Molecular dynamics (MD) and density functional theory (DFT), have already been used to compute surface energies and determine Wulff shapes for monoclinic M_3 C_3S [3–5]. In recent studies, molecular and dissociative adsorption of single water molecule were investigated on multiple surface planes of M_3 C_3S polymorph [6–8]. Zhang et al. have shown that the adsorption energy decreases with increasing amount of adsorbed molecules. Reactive MD studies indicates that after approximately 0.3 ns, the structural properties of the surface are lost, making further hydration process independent of the crystallographic surface plane, and driven by proton hopping mechanisms towards the bulk [3, 9]. No correlation was found between water adsorption energy and surface energy, when using

Email address: siham.kamali-bernard@insa-rennes.fr (Siham Kamali-Bernard)

static computational methods [3]. However, the proton diffusion after the initial stage of hydration was related to the location of the valence band maximum (VBM), which is mainly constituted of oxygen 2p orbitals [9, 10]. Previous DFT studies reveal that the local density of state of the VBM is close to the oxygen anions for C_3S, and close to oxygen in silicates for C_2S [11]. The higher reactivity of C_3S when compared to C_2S is explained by the difference in their electronic structure, arising from the presence of oxygen anions in C_3S. Calculations of a single water molecule sorption on a (100) surface of $T_1\,C_3S$, shown that chemisorption occured only in regions close to oxide ions. This behaviour was associated to the higher degree of freedom of oxide ions when compared to oxygen in silicate [9].

Proton transfer (PT) frequency strongly depends on hydrogen bonds (HB) fluctuation due to thermal motion [12], and thus cannot be analyzed by a 0 K, DFT investigation. Furthermore, such a phenomenon cannot be captured considering a single water molecule adsorption. A previous computational study found structural changes, as well as a huge increase in PT rate from a solid/water monolayer interface to a thicker water film [12]. Towards a better understanding of the C_3S/water interface, we performed an *ab initio* MD (AIMD) simulation, considering a water film thick enough to account for fluctuation of the HB network. AIMD is a powerful tool that has been used extensively to investigate the structural and dynamical behavior of water/oxide interfaces at the DFT level of theory [12–19]. However, only few AIMD studies were conducted on cementitious materials [20–22]. As far as we know, this is the first time that the very early hydration stage of C_3S is investigated using AIMD. In particular, the structure of water and the PT dynamics are analysed and quantified, and the results are compared with reactive molecular dynamics calculations, performed for that purpose.

2. Computational Methods

A simulation of the C_3S/water interface was performed on the symmetric, Ca-rich, (040) plane (as in [5]). The $M_3\,C_3S$ model employed was refined from XRD analysis by Mumme et al. [23]. The unit cell of 54 atoms was optimized, at the DFT level with the Quantum Espresso code, using the PBE exchange-correlation functional [24, 25] with a Grimme D2 correction for van der Waals interactions [26]. The kinetic energy cutoffs for wave functions and charge density were 45 Ry and 405 Ry, respectively. The Monkhorst-Pack method was used for the integration of the first Brillouin zone, with a $3 \times 3 \times 3$ k-point mesh. During the optimization process, the atoms were allowed to relax. In order to build a surface model, the optimized unit cell was converted to an orthorhombic supercell of 162 atoms, with lattice parameters $a = 12.28$ Å, $b = 7.09$ Å and $c = 25.59$ Å. This transformation was performed with the Atomsk code, which searches linear combination of the unit cell vectors producing vectors aligned with Cartesian axes [27]. The optimized monoclinic cell and corresponding orthorhombic supercell are represented in Fig. 1.

The surface model was created from three orthorhombic supercells, with a 20 Å thick vacuum layer, thus resulting in a 12.28 Å × 25.59 Å × 21.28 Å structure. The relaxation of the surface and the AIMD simulation were performed with the CP2K code, using a PBE functional, and a combination of Gaussian and plane wave basis functions (GPW), with Grimme D2 correction. A 400 Ry planewave cutoff was adopted, and the reciprocal space was sampled only at the γ point. To relax the surface, the periodicity was applied for in-plane directions, and removed in the direction of the vacuum. The atoms of the surface were allowed to relax at the DFT level, ensuring that almost no change occurs within the middle of the slab. The interface model was created adding a 15 Å thick layer of water (157 molecules), with a 15 Å vacuum region. The structure of the $C_3S(040)$/water interface is depited in Fig. 2.

While the atoms of the mineral surface were kept fixed,

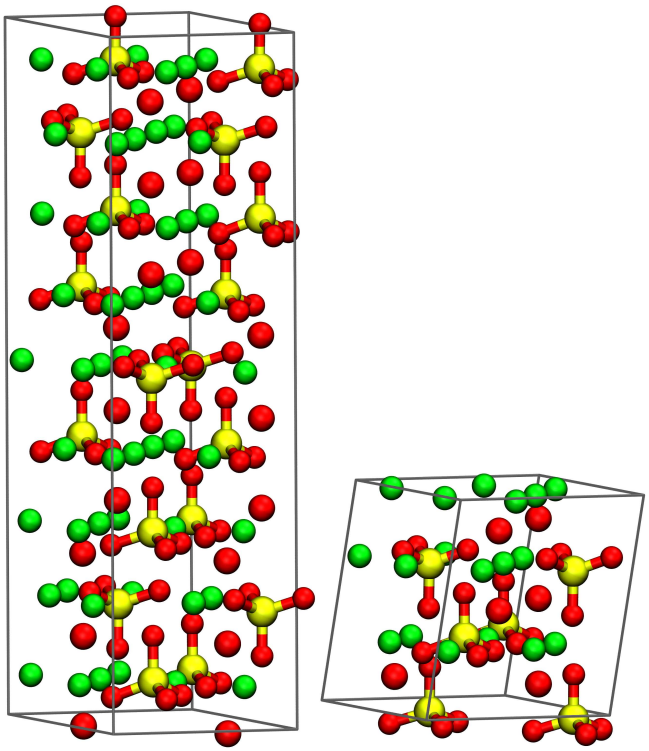

Figure 1: M_3 monoclinic cell, optimized from the model by Mumme et al. [23] (right). Corresponding orthorhombic supercell (left). Color code: calcium cations in green, oxygen anions and silicate oxygen in red, silicon atoms in yellow.

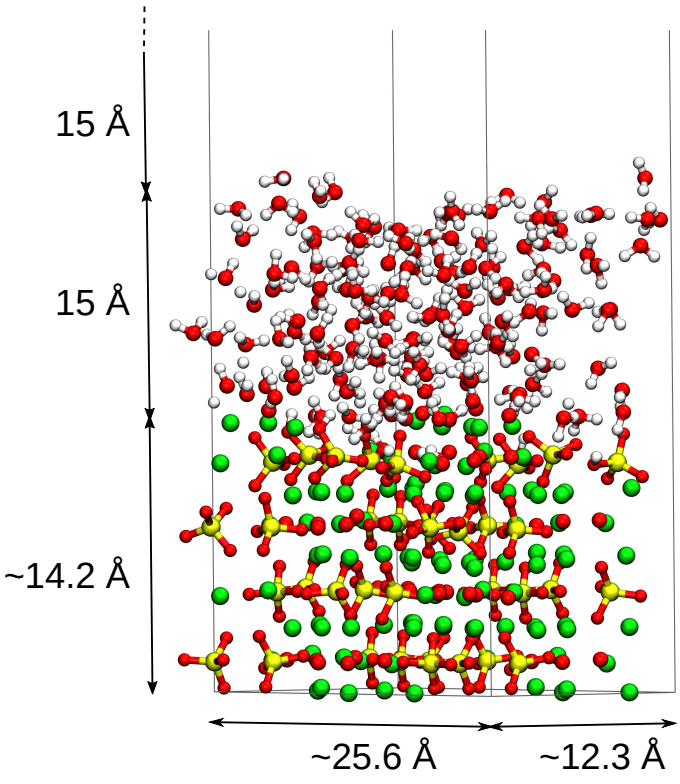

Figure 2: Structure of the investigated $C_3S(040)$/water interface.

the water molecules were allowed to relax on the surface during a 2 ns classical MD run in NVT ensemble at 300 K, using the INTERFACE FF parameters for C_3S [5] and a SPC model for water [28]. In order to minimize the computational time, the bottom layer was removed so that the remaining slab was composed of two orthorhombic supercells (∼14 Å thick) and during the AIMD run, the lower supercell, considered as the bulk, was fixed. Afterwards, a 18 ps AIMD run was performed within the Born-Oppenheimer approximation, in the canonical ensemble, with a Nose-Hoover thermostat, integrating the equation of motion with a 0.5 fs timestep. Based on the evolution of the energy of the system, it was considered that the equilibrium was reached after 6 ps, and the remaining simulation time was used for analysis of equilibrium properties. A slightly higher temperature of 360 K (compared to standard conditions) was used to balance the low diffusivity of water using the PBE functional. Deuterium masses were used for protons to minimize the vibrational frequency of nuclei. It deserves to highlight that such substitution could decrease the frequency of PT, because of the lower vibrational frequency of deuterium nuclei in comparison to hydrogen nuclei. However, this method has already been used in the literature to prevent from energy drifts and it is understood that its benefits outweigh losses [12, 29]. A reactive molecular dynamics simulation was performed using the ReaxFF, with the current optimized set of parameters for Ca/O/H/Si elements [30–32]. The simulation method and parameters, as well as the system size, are in accordance with previously reported calculations [3].

3. Results

3.1. Water structure

In this article, Oi refers to oxygen anions, Os refers to oxygens in silicates, and Odw refers to oxygens resulting from the dissociation of water molecules. At the very first steps of the simulation, three oxide ions Oi from equivalent sites are protonated. The hydration model for C_3S

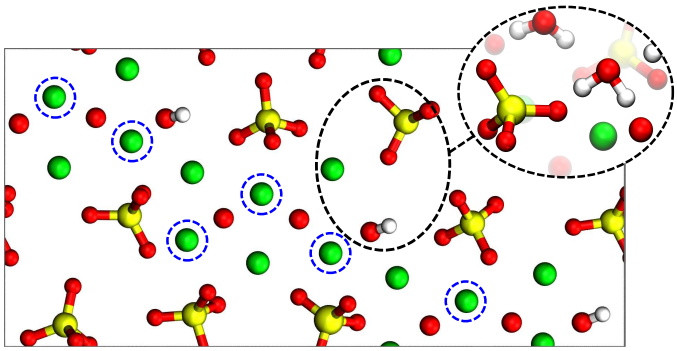

Figure 3: Atomic structure of the (040) surface. Hydrogen in hydroxide H-Oi are colorized in white. The snapshot shows the position of the water molecule before protonation of the oxide ion. The ions of the surface are in the same layer, except for the calcium indicated by blue circles, having perpendicular coordinate z ∼2 Å larger.

proposed by Pustovgar et al. considers that protonation of oxide ions occurs before protonation of silicates [33]. Although hydroxides are more stable than silanol groups, our simulation indicates that on the considered (040) Ca-rich surface, protonation of Oi only occurs on sites close to silicates. The other superficial oxide ions are shielded by four calcium cations, hindering any protonation reaction. The negatively charged region allows water molecules to form hydrogen bonds with oxide ions on one side and with oxygens in silicates on the other side, thus leading to protonation of Oi (see Fig. 3).

The number of H-Os groups formed on silicates tends to stabilize after ∼1 ps whereas the number of H-Odw groups stabilize after ∼0.25 ps (see Fig. 4). Both hydroxyl groups fluctuate during the whole simulation due to proton transfer. Conversely, the hydroxides H-Oi formed on oxygen anions Oi are very stable and no backward PT occurs. From our simulation using the ReaxFF, within the timescale of 18 ps, a steady state is reached very quickly as in the AIMD simulation. However, all hydroxyl groups formed in the ReaxFF simulation are very stable, and the currently developed set of parameters for Ca/O/H/Si failed to describe the PT dynamics between water and Oi/Os atoms which is observed in our AIMD simulation. The complexity to optimize parameters for ReaxFF relies on the fact that the same set of parameters is employed for each element [34]. It means that the parameters are the same independently of the environment. Other approaches based on the empirical valence bond model has succeeded in reproducing OH^- solvation and transport in water solutions [35]. The implementation of a PT model almost doubled the diffusion of OH^- ions when compared to a classical model. The hydroxyl coverage of each hydroxyl type is close to the result of the AIMD simulation. Therefore, within the timescale of the simulation, the ReaxFF is representing the protonation state of the (040) surface in good agreement with the AIMD simulation. The average total hydroxyl coverage over the last 12 ps of simulation is $(5.36 \pm 0.37)\,\mathrm{HO/nm^2}$ for the AIMD simulation, and $(5.17 \pm 0.01)\,\mathrm{HO/nm^2}$ for the ReaxFF simulation. These values are also in agreement with previous investigation on C_3S hydration, using the ReaxFF [3, 9].

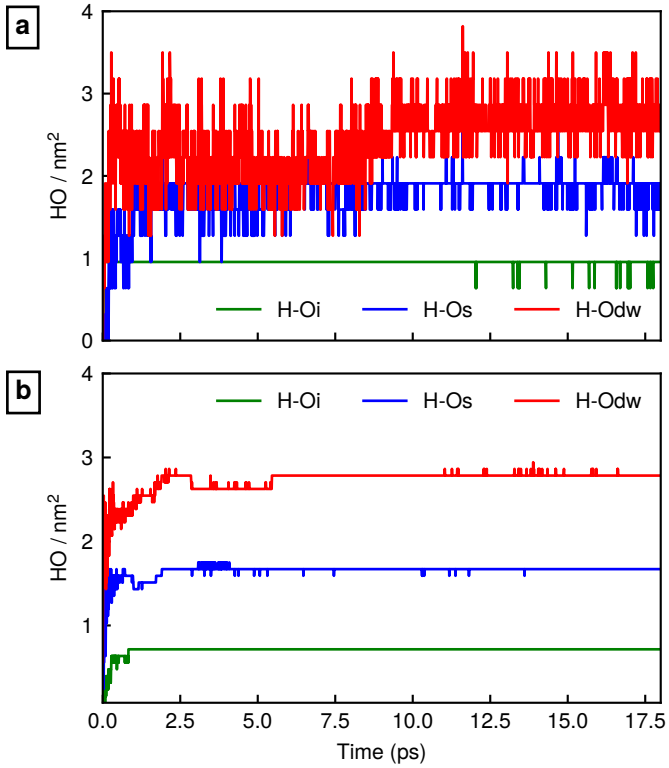

Figure 4: Number of hydroxyl groups formed at the surface on oxide ions (Oi-H), oxygen in silicates (Os-H), and from water dissociation (Odw-H) for (a) AIMD simulation, (b) ReaxFF simulation.

The atomic density profile of water oxygen and hydrogen atom, along the axis perpendicular to the surface, is reported in Fig. 5. The layered structure of the interfacial water results from the effect of excluded volume, electrostatic force field, and hydrogen bonding network. Previous investigations based on classical MD simulations showed that this layering is lost with protonation of the surface [36]. The closest hydrogen's peak from the surface, is at the average position of oxygen in silicates Os ($z = 0$), and corresponds to chemisorbed H. The thickness of the layered region is approximately the same as in our previous classical MD investigation: ∼5–6 Å [36].

The radial distribution functions (RDF) of H-Oi, H-Os and Ow-Ca pairs are plotted in Fig. 6.

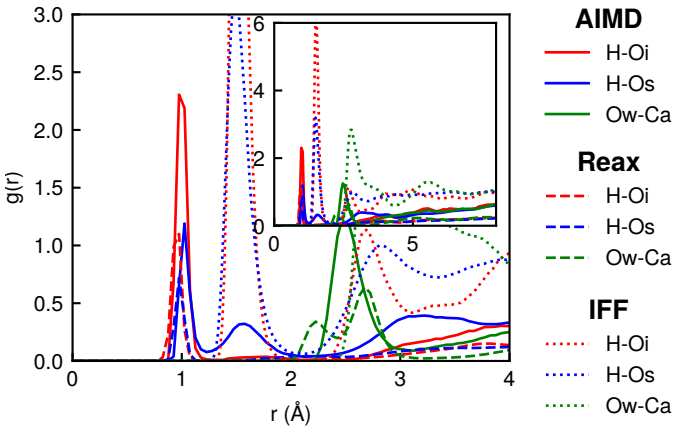

Figure 6: Radial distribution function H-Oi, H-Os, and Ow-Ca pairs employing AIMD, ReaxFF, and IFF [36]. The inset shows a zoom out (×0.5).

For H-Oi and Ow-Ca pairs, sharp peaks raise at ∼0.97 Å and ∼2.50 Å respectively, indicating superficial hydroxides and the first coordination shell of calcium cation. No second coordination shell is noticed for both pairs. Yet for the H-Os pairs, two peaks stand at ∼1.02 Å and ∼1.58 Å, corresponding to hydroxyl groups formed on silicates and H-bonds between water and oxygen in silicates. The RDF obtained in the ReaxFF simulation is very similar, with two main differences: in one case, only one correlation peak is observed for the H- Os pair, suggesting an Os protonation, and the coordination peak for Ow-Ca pairs is split in two, indicating two different distances of correlated water molecules. RDF for dry C_3S/water interface, obtained from previous MD investigation [36], was plotted for comparative purpose. In such classical simulation, no PT occurs and the first coordination peak correspond to H-bonds between water and superficial anions (r ∼1.53 Å).

The orientation of water molecules in contact with the surface is a characteristic of the hydrophilic/hydrophobic behavior of the surface. The probability distribution of the angle θ between the water dipole moment and the z axis is depicted in Fig. 7 a). Within the contact layer (z <1.6 Å), most of the water molecules have θ ∼20–50° or θ ∼120–160°, meaning that their dipole moments point preferentially towards or against the surface. This feature is characteristic of hydrophilic surfaces [37]. Less probably, water molecules forming a single hydrogen bond with silicates orient with their dipole moment parallel to the surface. Water molecules in the contact layer orient according to the charge of superficial ionic species. Thus, two regions can be distinguished: one where the water dipole is oriented upward and H atoms coordinate with Os, and a second where the water dipole is oriented downward and Ow atoms coordinate with calcium cations. These regions are mapped on the surface in Fig. 7 b) by collecting θ and the x and y coordinates of water molecules within 3 Å from the surface, during the whole simulation. The effect of the topology of C_3S surfaces on the structure of water molecules has already been reported in a previous molecular dynamics investigation [38].

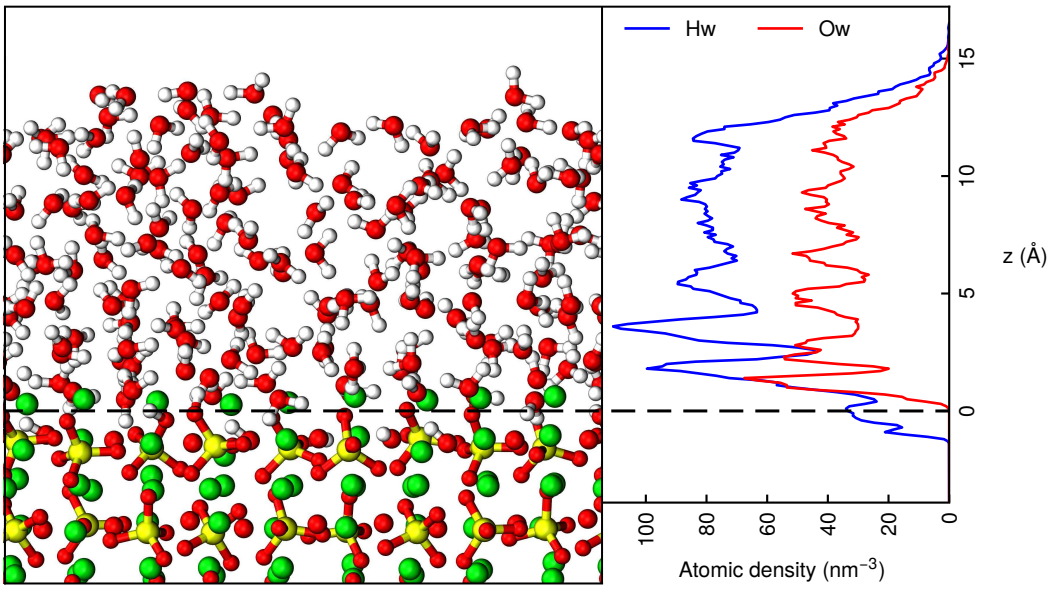

Figure 5: Atomic density profile of water molecules along the z axis for AIMD. The origin adopted is the average coordinate of the uppermost oxygen silicate layer. The layering observed results from the hydrogen bond network created between the strong interaction between the water molecules and the ionic surface.

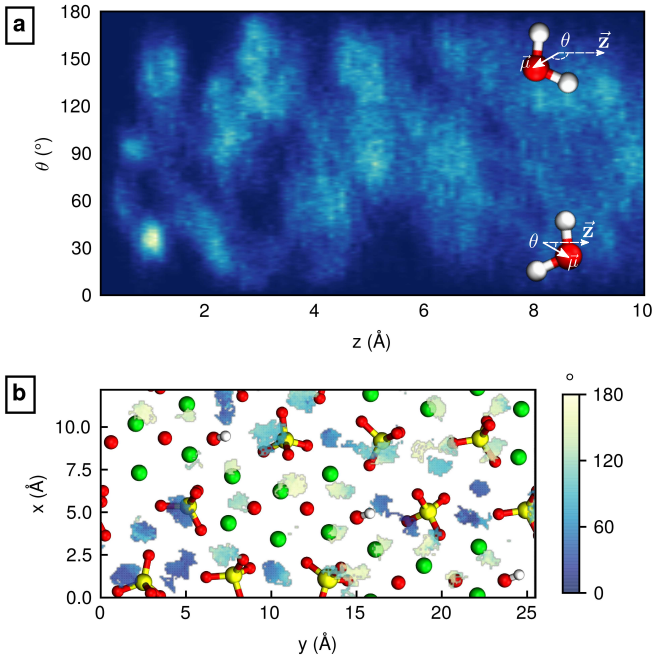

Figure 7: (a) Probability distribution of the angle θ between the water dipole moment and the z axis, perpendicular to the surface. Lighter regions correspond to higher probabilities (b) Density mapping of θ for water molecules within 3 Å from the surface. Color code: Ca in green, Os and Oi in red, Si in yellow, H in hydroxide H-Oi in white.

The probability distribution of H-Os and H-Odw hydroxyl groups is plotted in Fig. 8. H-Odw groups are principally located on Ca-rich, positively charged regions, but also close to protonated silicates.

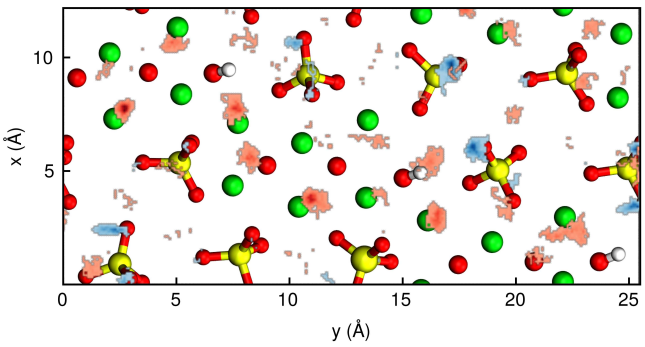

Figure 8: Normalized probability distribution of H-Os (blue) and H-Odw (red) hydroxyl groups.

3.2. Proton transfer analysis

The frequency ν of PT between water molecules and Os-H and Odw-H groups is reported in Fig. 9. The lifetime τ is defined as the time for a proton to return to the oxygen atoms to which it was initially bonded.

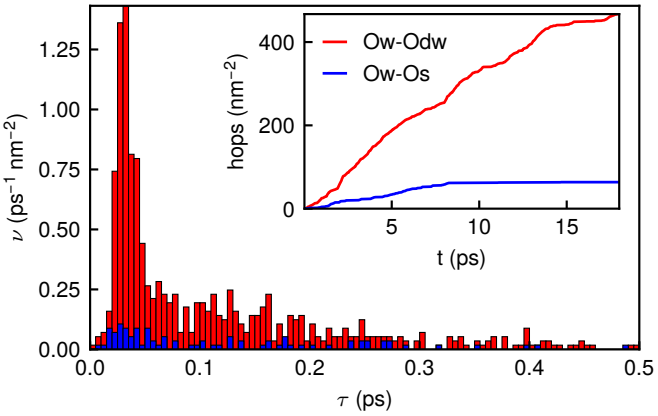

Figure 9: Frequency ν of PT as a function of its lifetime τ (left). Evolution of the total number of hops within the simulation time (right).

The inset plot shows the evolution of proton hops during the simulation. Hops between Ow and Os reach a plateau after ∼8 ps. Conversely, hops within Odw-Ow pairs seems to increase steadily during the whole simulation and are about 5 times more frequent than within Os-Ow pairs during the first 8 ps. The typical lifetime of PT events is shorter than 100 fs, which corresponds to the time scale of Eigen-Zendel structure interchanging in bulk water, obtained by femtosecond vibrational spectroscopy [39]. Lifetimes of approximately the same duration were reported for PT at water/ZnO($10\bar{1}0$) interface [12]. The longest lifetimes reported are ∼0.2 ps for transfer between Ow and Os, and ∼2 ps for transfer between Ow and Odw.

The free energy profiles of PT between Ow and Os and between Ow and Odw pairs were obtained from a standard method as follows: $F = -k_B T \log P$ (see Fig. 10) [12, 35, 40]. P is a probability distribution function of the distance $d_{\text{Oa-Ob}}$ between two oxygen atoms Oa and Ob, and of $\delta_{\text{a-b}} = d_{\text{Oa-H}} - d_{\text{Ob-H}}$. In the case of PT between Ow and Os, the molecular configuration of water forming an H-bond with Os is more stable than the dissociative configuration. The free energy profile of PT between Ow and Odw suggests that the molecular adsorption of water on the surface is more stable than the dissociated form. This observation is contrary to previous DFT and reactive MD calculations on a single water molecule, where dissociative adsorption energies were generally larger than molecular adsorption energies, resulting in more stable configurations [3, 6–8]. This consolidates the idea that static calculations on single molecule adsorption cannot describe accurately the properties of a solid/water interface. Tocci and Michaelides also reported considerable differences in PT rate between a monolayer and an thicker water film [12]. These differences arise from the decrease of the free energy barrier of proton transfers induced by H-bond fluctuations. The free energy barrier is ∼3.24 k_BT for PT from Ow to Os and ∼2.24 k_BT from Os to Ow. The barrier is ∼3.30 k_BT for transfer from Ow to Odw and ∼3.60 k_BT for the reverse reaction. These results suggest that hydroxides formed by water dissociation are more stable than silanol groups. However, the energy barrier for the creation of both hydroxyl groups is almost equal.

Electron density difference analysis allows to map the distribution of electrons involved in PT, and more generally in the adsorption. This analysis was realized performing static DFT calculation on the total system, as well as C_3S, and water independently on the system configuration at 5 ps. The electron density difference $\Delta\rho$ was calculated as follow:

$$\Delta\rho = \rho_{C_3S/H_2O} - \rho_{C_3S} - \rho_{H_2O} \quad (1)$$

where ρ_{C_3S/H_2O} corresponds to the electron density of the interface system, ρ_{C_3S} and ρ_{H_2O} are the electron density of the C_3S and water alone, respectively. A positive value of $\Delta\rho$ indicates a high electron density, while a negative value points out an electron depletion region.

The proton transfers occurring at the surface create an electron delocalization, and thus high and low electron density regions. Water molecules act as charge carrier and the electron depletion or gain highly depends on the location of the molecule (see Fig. 11 a and b1). High electron density is observed around the silicate oxygen close to the water molecule, creating a depletion region on the

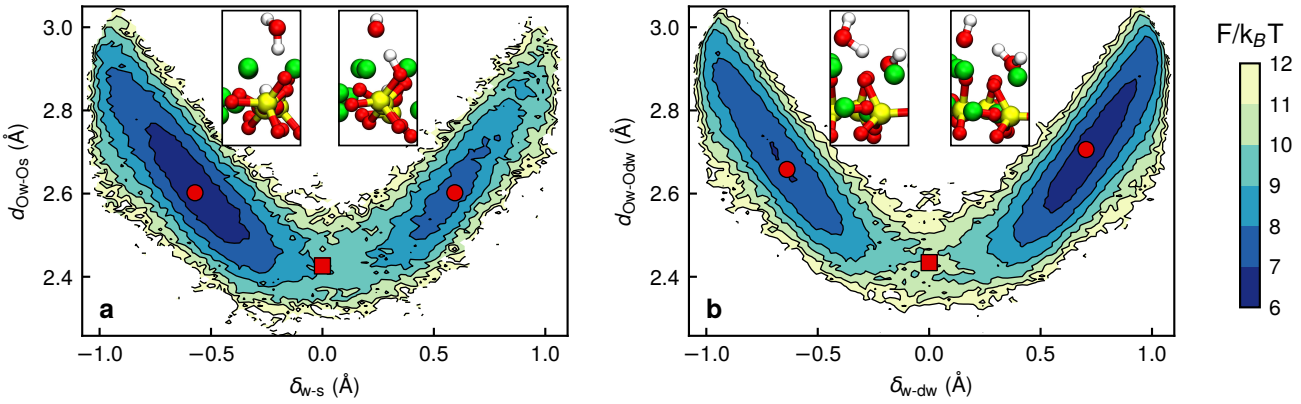

Figure 10: Free energy contour plot of PT between Ow and Os as a function of the distance $d_{\text{Oa-Ob}}$ between oxygen atoms, and of $\delta_{\text{a-b}} = d_{\text{Oa-H}} - d_{\text{Ob-H}}$. The red circles shows the local free energy minima, corresponding to the most stable configurations before and after the proton jump. The red square is the saddle point, where the proton is equidistant from both oxygen atoms.

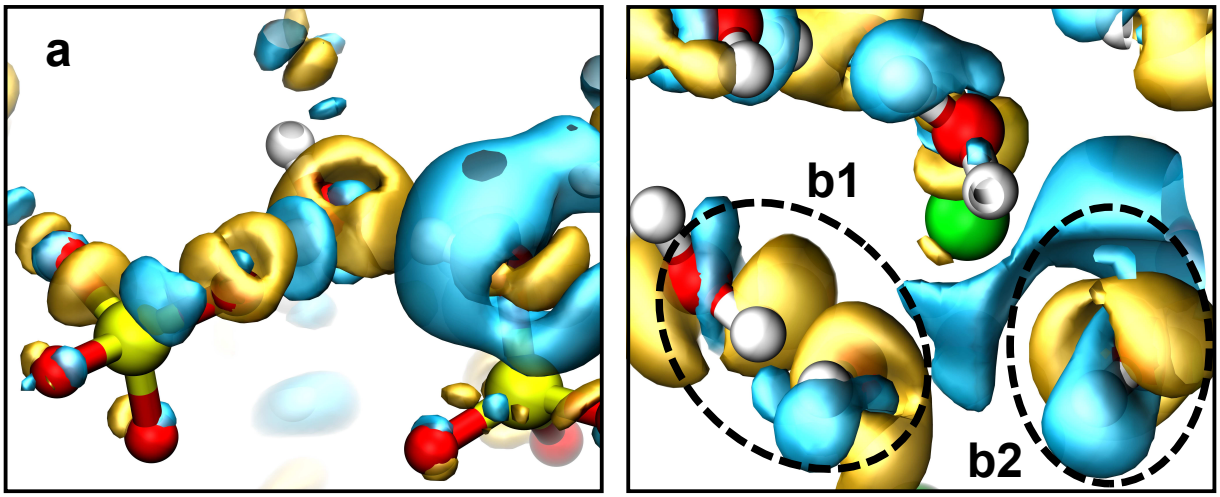

Figure 11: Snapshots of the isosurface of electron density difference. Golden and cyan isosurface represent positive and negative $\Delta\rho$, respectively. a) A water molecule between a silicate and a silanol group. b1) Electron density delocalization during a proton exchange between a molecular water and a hydroxide. b2) Electron abundance and depletion regions around an hydroxide created upon water dissociation.

silicon atom. A large depletion region is observed around the silanol group (Fig. 11 a). Charge depletion regions are observed around H of hydroxyl groups. Their magnitude increase in this order: H-Oi < H-Odw < H-Os. In other words, the magnitude of the depletion regions on H decreases as a function of the stability of the hydroxyl group. A large depletion region indicates a greater charge separation, and a more ionic bond, while a small depletion region reveals a more covalent bond.

4. Conclusion

The very early hydration of the (040) surface of C_3S was investigated through a 18 ps AIMD simulation. As a first observation, only 1/3 of the oxide ions on the surface were protonated during the whole simulation. The hydroxides formed are highly stable and no proton exchange was observed. Although the oxide ion is very unstable in water, we found that its environment on the surface is an important factor for the creation of hydrogen bond with water molecules and for protonation to occur. Thus, the pKa of hydroxide and silicic acid in solution cannot predict accurately the protonation state of the surface during the very early stage of hydration. The structure of water at the interface, resulting from the formation of the hydrogen bond network, is very similar to that of our previous classical molecular dynamics study, with a thickness of the layered region of approximately 5–6 Å from the surface. The (040) surface is composed of Ca-rich regions (positively charged) and Si-rich regions (negatively charged). Water molecules in the contact layer orient their dipole moment in accordance with the surface charge, making either H-bonds in Si-rich regions, or creating strong Ca-Ow interactions in Ca-rich regions. Energy barrier analysis suggests that the molecular adsorption of water on the C_3S surface is more stable than dissociative adsorption. Based on proton transfer energy analysis, the hydroxyl groups formed were classified in order of stability as follow: H-Oi > H-Odw > H-Os. From electron density difference, high electron density, and depletion regions were observed. These observations revealed that the magnitude of the electron depletion region upon adsorption is smaller for more stable hydroxyl groups.

Acknowledgments

The authors acknowledge Brazilian science agencies CAPES (PDSE process n°88881.188619/2018-01) and CNPq for financial support, as well as Hegoi Manzano and Gabriele Tocci for helpful discussions. The authors also thank the anonymous reviewers for their careful reading of our manuscript and their many insightful comments and suggestions.

References

[1] J. W. Bullard, H. M. Jennings, R. A. Livingston, A. Nonat, G. W. Scherer, J. S. Schweitzer, K. L. Scrivener, J. J. Thomas, Mechanisms of cement hydration, Cement and Concrete Research 41 (12) (2011) 1208–1223. doi:10.1016/j.cemconres.2010.09.011.

[2] R. K. Mishra, A. K. Mohamed, D. Geissbühler, H. Manzano, T. Jamil, R. Shahsavari, A. G. Kalinichev, S. Galmarini, L. Tao, H. Heinz, R. Pellenq, A. C. van Duin, S. C. Parker, R. J. Flatt, P. Bowen, cemff : A force field database for cementitious materials including validations, applications and opportunities, Cement and Concrete Research 102 (2017) 68–89. doi:10.1016/j.cemconres.2017.09.003.

[3] H. Manzano, E. Durgun, I. López-Arbeloa, J. C. Grossman, Insight on Tricalcium Silicate Hydration and Dissolution Mechanism from Molecular Simulations, ACS Applied Materials & Interfaces 7 (27) (2015) 14726–14733. doi:10.1021/acsami.5b02505.

[4] E. Durgun, H. Manzano, P. V. Kumar, J. C. Grossman, The Characterization, Stability, and Reactivity of Synthetic Calcium Silicate Surfaces from First Principles, The Journal of Physical Chemistry C 118 (28) (2014) 15214–15219. doi:10.1021/jp408325f.

[5] R. K. Mishra, R. J. Flatt, H. Heinz, Force Field for Tricalcium Silicate and Insight into Nanoscale Properties: Cleavage, Initial Hydration, and Adsorption of Organic Molecules, The Journal of Physical Chemistry C 117 (20) (2013) 10417–10432. doi:10.1021/jp312815g.

[6] Y. Zhang, X. Lu, D. Song, S. Liu, The adsorption behavior of a single and multi-water molecules on tricalcium silicate (111)

surface from DFT calculations, Journal of the American Ceramic Society (2018). doi:10.1111/jace.16093.

[7] Y. Zhang, X. Lu, D. Song, S. Liu, The adsorption of a single water molecule on low-index C_3S surfaces: A DFT approach, Applied Surface Science 471 (2019) 658–663. doi:10.1016/j.apsusc.2018.12.063.

[8] C. Qi, L. Liu, J. He, Q. Chen, L.-J. Yu, P. Liu, Understanding Cement Hydration of Cemented Paste Backfill: DFT Study of Water Adsorption on Tricalcium Silicate (111) Surface, Minerals 9 (4) (2019) 202. doi:10.3390/min9040202.

[9] J. Huang, B. Wang, Y. Yu, L. Valenzano, M. Bauchy, G. Sant, Electronic Origin of Doping-Induced Enhancements of Reactivity: Case Study of Tricalcium Silicate, The Journal of Physical Chemistry C 119 (46) (2015) 25991–25999. doi:10.1021/acs.jpcc.5b08286.

[10] J. Huang, L. Valenzano, T. V. Singh, R. Pandey, G. Sant, Influence of (Al, Fe, Mg) Impurities on Triclinic Ca_3SiO_5: Interpretations from DFT Calculations, Crystal Growth & Design 14 (5) (2014) 2158–2171. doi:10.1021/cg401647f.

[11] E. Durgun, H. Manzano, R. J. M. Pellenq, J. C. Grossman, Understanding and Controlling the Reactivity of the Calcium Silicate phases from First Principles, Chemistry of Materials 24 (7) (2012) 1262–1267. doi:10.1021/cm203127m.

[12] G. Tocci, A. Michaelides, Solvent-Induced Proton Hopping at a Water-Oxide Interface, The Journal of Physical Chemistry Letters 5 (3) (2014) 474–480. doi:10.1021/jz402646c.

[13] O. Björneholm, M. H. Hansen, A. Hodgson, L.-M. Liu, D. T. Limmer, A. Michaelides, P. Pedevilla, J. Rossmeisl, H. Shen, G. Tocci, E. Tyrode, M.-M. Walz, J. Werner, H. Bluhm, Water at Interfaces, Chemical Reviews 116 (13) (2016) 7698–7726. doi:10.1021/acs.chemrev.6b00045.

[14] B. F. Ngouana-Wakou, P. Cornette, M. C. Valero, D. Costa, P. Raybaud, An Atomistic Description of the γ-Alumina/Water Interface Revealed by Ab Initio Molecular Dynamics, The Journal of Physical Chemistry C 121 (19) (2017) 10351–10363. doi:10.1021/acs.jpcc.7b00101.

[15] J. M. Rimsza, J. Yeon, A. C. T. van Duin, J. Du, Water Interactions with Nanoporous Silica: Comparison of ReaxFF and ab Initio based Molecular Dynamics Simulations, The Journal of Physical Chemistry C 120 (43) (2016) 24803–24816. doi:10.1021/acs.jpcc.6b07939.

[16] Á. Cimas, F. Tielens, M. Sulpizi, M.-P. Gaigeot, D. Costa, The amorphous silica–liquid water interface studied by ab initio molecular dynamics (AIMD): local organization in global disorder, Journal of Physics: Condensed Matter 26 (24) (2014) 244106. doi:10.1088/0953-8984/26/24/244106.

[17] S. Laporte, F. Finocchi, L. Paulatto, M. Blanchard, E. Balan, F. Guyot, A. M. Saitta, Strong electric fields at a prototypical oxide/water interface probed by ab initio molecular dynamics: MgO(001), Physical Chemistry Chemical Physics 17 (31) (2015) 20382–20390. doi:10.1039/c5cp02097b.

[18] M.-S. Lee, B. P. McGrail, R. Rousseau, V.-A. Glezakou, Structure, dynamics and stability of water/scCO2/mineral interfaces from ab initio molecular dynamics simulations, Scientific Reports 5 (1) (2015). doi:10.1038/srep14857.

[19] L. Liu, M. Krack, A. Michaelides, Density Oscillations in a Nanoscale Water Film on Salt: Insight from Ab Initio Molecular Dynamics, Journal of the American Chemical Society 130 (27) (2008) 8572–8573. doi:10.1021/ja8014296.

[20] S. V. Churakov, Structure of the interlayer in normal 11 Å tobermorite from an ab initio study, European Journal of Mineralogy European Journal of Mineralogy 21 (1) (2009) 261–271. doi:10.1127/0935-1221/2009/0021-1865.

[21] S. V. Churakov, Structural position of H2O molecules and hydrogen bonding in anomalous 11 A tobermorite, American Mineralogist 94 (1) (2009) 156–165. doi:10.2138/am.2009.2907.

[22] S. V. Churakov, C. Labbez, Thermodynamics and Molecular Mechanism of Al Incorporation in Calcium Silicate Hydrates, The Journal of Physical Chemistry C 121 (8) (2017) 4412–4419. doi:10.1021/acs.jpcc.6b12850.

[23] W. G. Mumme, Crystal structure of tricalcium silicate from a Portland cement clinker and its application to quantitative XRD analysis, Neues Jahrbuch fuer Mineralogie: Monatshefte 4 (1995) 145–160.

[24] J. P. Perdew, K. Burke, M. Ernzerhof, Generalized Gradient Approximation Made Simple, Physical Review Letters 77 (18) (1996) 3865–3868. doi:10.1103/physrevlett.77.3865.

[25] J. P. Perdew, K. Burke, M. Ernzerhof, Generalized Gradient Approximation Made Simple [Phys. Rev. Lett. 77, 3865 (1996)], Physical Review Letters 78 (7) (1997) 1396–1396. doi:10.1103/physrevlett.78.1396.

[26] S. Grimme, Semiempirical GGA-type density functional constructed with a long-range dispersion correction, Journal of Computational Chemistry 27 (15) (2006) 1787–1799. doi:10.1002/jcc.20495.

[27] P. Hirel, Atomsk: A tool for manipulating and converting atomic data files, Computer Physics Communications 197 (2015) 212–219. doi:10.1016/j.cpc.2015.07.012.

[28] H. J. C. Berendsen, J. P. M. Postma, W. F. van Gunsteren, J. Hermans, Interaction Models for Water in Relation to Protein Hydration, in: The Jerusalem Symposia on Quantum Chemistry and Biochemistry, Springer Netherlands, 1981, pp. 331–342. doi:10.1007/978-94-015-7658-1_21.

[29] K. Leung, S. B. Rempe, Ab initio rigid water: Effect on water structure, ion hydration, and thermodynamics, Physical Chemistry Chemical Physics 8 (18) (2006) 2153. doi:

10.1039/b515126k.

[30] J. C. Fogarty, H. M. Aktulga, A. Y. Grama, A. C. T. van Duin, S. A. Pandit, A reactive molecular dynamics simulation of the silica-water interface, The Journal of Chemical Physics 132 (17) (2010) 174704. doi:10.1063/1.3407433.

[31] H. Manzano, R. J. M. Pellenq, F.-J. Ulm, M. J. Buehler, A. C. T. van Duin, Hydration of Calcium Oxide Surface Predicted by Reactive Force Field Molecular Dynamics, Langmuir 28 (9) (2012) 4187–4197. doi:10.1021/la204338m.

[32] H. Manzano, S. Moeini, F. Marinelli, A. C. T. van Duin, F.-J. Ulm, R. J.-M. Pellenq, Confined Water Dissociation in Microporous Defective Silicates: Mechanism, Dipole Distribution, and Impact on Substrate Properties, Journal of the American Chemical Society 134 (4) (2012) 2208–2215. doi:10.1021/ja209152n.

[33] E. Pustovgar, R. K. Mishra, M. Palacios, J.-B. d'Espinose de Lacaillerie, T. Matschei, A. S. Andreev, H. Heinz, R. Verel, R. J. Flatt, Influence of aluminates on the hydration kinetics of tricalcium silicate, Cement and Concrete Research 100 (2017) 245–262. doi:10.1016/j.cemconres.2017.06.006.

[34] T. P. Senftle, S. Hong, M. M. Islam, S. B. Kylasa, Y. Zheng, Y. K. Shin, C. Junkermeier, R. Engel-Herbert, M. J. Janik, H. M. Aktulga, T. Verstraelen, A. Grama, A. C. T. van Duin, The ReaxFF reactive force-field: development, applications and future directions, npj Computational Materials 2 (2016). doi:10.1038/npjcompumats.2015.11.

[35] I. S. Ufimtsev, A. G. Kalinichev, T. J. Martinez, R. J. Kirkpatrick, A multistate empirical valence bond model for solvation and transport simulations of OH- in aqueous solutions, Physical Chemistry Chemical Physics 11 (41) (2009) 9420. doi:10.1039/b907859b.

[36] J. Claverie, F. Bernard, J. M. M. Cordeiro, S. Kamali-Bernard, Water's behaviour on Ca-rich tricalcium silicate surfaces for various degrees of hydration: A molecular dynamics investigation, Journal of Physics and Chemistry of Solids (2019). doi:10.1016/j.jpcs.2019.03.020.

[37] B. V. Deryagin, N. V. Churaev, Structure of water in thin layers, Langmuir 3 (5) (1987) 607–612. doi:10.1021/la00077a002.

[38] A. Alex, A. K. Nagesh, P. Ghosh, Surface dissimilarity affects critical distance of influence for confined water, RSC Adv. 7 (6) (2017) 3573–3584. doi:10.1039/c6ra25758e.

[39] S. Woutersen, H. J. Bakker, Ultrafast Vibrational and Structural Dynamics of the Proton in Liquid Water, Physical Review Letters 96 (13) (2006). doi:10.1103/physrevlett.96.138305.

[40] Z. Zhu, M. E. Tuckerman, Ab Initio Molecular Dynamics Investigation of the Concentration Dependence of Charged Defect Transport in Basic Solutions via Calculation of the Infrared Spectrum†, The Journal of Physical Chemistry B 106 (33) (2002) 8009–8018. doi:10.1021/jp020866m.